2011 American Control Conference
on O'Farrell Street, San Francisco, CA, USA
June 29 - July 01, 2011

Design of Reduced Order Sliding Mode Governor for Hydro-turbines

Dianwei Qian, Jianqiang Yi, *Senior Member, IEEE*, and Xiangjie Liu

Abstract— **This paper investigates modeling and control problems of the speed governing system of a hydro-generator unit with one upstream surge tank, driven by a Francis turbine. This governing system is organized into four main functional blocks, namely the hydrodynamic, mechanical, electrical, and servo subsystems. Mathematic models of the individual components are developed and are subsequently interconnected to obtain a model for the governor design. From the viewpoint of modern control theory, only a part of states of this speed governing system are measurable. By introducing an additional state variable, a reduced order sliding mode controller is presented. Simulation results illustrate the feasibility and robustness of the presented method.**

I. Introduction

WITH the coming of low carbon epoch, low-carbon power generation will be realized by developing and popularizing zero-emission thermal power generation, advanced atomic power generation, renewable energy, *e tc* [1]. As a kind of zero-carbon generation form, hydropower, currently accounting for 19% of global electricity generated from primary sources [1], offers an important low-carbon energy solution.

Generally speaking, a typical hydroelectric power plant is made up of reservoir, water tunnel, surge tank, penstock, hydraulic turbine, speed governor, generator, and grid [2]. This system possesses strong couplings between hydraulic and mechano-electric dynamics. Due to the existence of different operating conditions, the system characteristics will change the moment that operating condition changes [3]. These undesired properties trouble the governor design of this complex system.

As Kishor *et al* [2] pointed out that a key item of any hydro power plant was its governor, many approaches concerning the governor design problem of hydro-generator units have been reported in the last three decades. Two classes of the governors can be roughly seen. The first class is with the proportional-integral-derivative (PID) or PID-type governor, [3], [4] and [5], the other with the state feedback or intelligence-based governor, [6], [7] and [8].

Since the PID governor methodology only focuses on the system output and harnesses the information of the current error (P), the sum of errors in history (I), the rate at which the error has been changing (D), this methodology would lose the inner information of this system. Moreover, such the PID governor is designed at one load condition and is re-tuned for the worst operating condition, which does not ensure the governing system is stable under all operating conditions. Modern control theory not only employs the system output, but also uses the system inner states to decide the final control input. With the development of modern control approaches, *e.g.* predictive control [6], intelligent method control [7], robust control [9], multi-model control [10], *e tc*, these methods are now being turned to practical accounts of the governor design of hydroelectric turbines.

Sliding mode control (SMC)is a form of variable structure control (VSC) [11]. It is a nonlinear feedback control method that alters the dynamics of a nonlinear system by application of a high-frequency switching control. It switches from one continuous structure to another based on the current position in state space so that the system trajectories always move toward a switching condition and the ultimate trajectory will slide along the boundaries of the control structures. The geometrical locus consisting of the boundaries is called the sliding (hyper)surface. The motion taking place on the surface is called a sliding mode. The main strength of SMC is its robustness. It is insensitive to parameter variations and extraneous disturbance that enter into the control channel. Additionally, the sliding mode is reached in finite time, *i.e.*, better than an asymptotic behavior. This nonlinear method offers an alternative method to solve the speed control problem of hydroelectric turbines. In [12] – [14], variable structure control methods with no sliding mode were turned into practical accounts for governing the hydroelectric turbine speed. So far, there has been rather rare literature about the applications of SMC on this field.

This paper investigates a new approach for the speed control of hydro-turbines by means of SMC. After modelling the speed governing system of a hydroelectric power plant with one upstream surge tank, a reduced-order sliding mode controller is proposed. To validate the feasibility and robustness of the control method, simulation results are illustrated. The reminder of this paper is organized as follows. In Section 2, the dynamic model of the speed governing system is depicted. The reduced-order sliding mode control law is designed in Section 3. The presented method in Section 4 is taken into practical accounts to verify the controller's feasibility and robustness. Finally, conclusions are drawn in Section 5.

II. Dynamic Model

In [15], a linear model of speed governing system was taken for a low-to-medium head plant with either a very

This work was supported by the NSFC Projects under grant No. 60904008, 60975060, 60974051, the Fundamental Research Funds for the Central Universities under grant No. 09MG19.

D.W. Qian and X.J. Liu are with the School of Control and Computer Engineering, North China Electric Power University, Beijing, 102206, P.R. China. Email: dianwei.qian@ncepu.edu.cn

J.Q. Yi is with Institute of Automation, Chinese Academy of Sciences, Beijing, 100190, P.R.China.

large or no surge tank, which involved no surge tank part. In the referred papers, most of them [4] – [14] took this model to verify their control methods. But the model neglected the effect of a surge tank and may deteriorate the accuracy of the system performance. Though Fang *et al* [3] reported a model of hydro power plants with two surge tanks, more than half of hydroelectric power plants are only with one surge tank at their upstream tunnels. In this section, we will capture the dynamic model of hydropower plants with only one upstream surge tank.

Fig. 1 displays the schematic diagram of the hydraulic installation of a hydroelectric power plant with one upstream surge tank. The symbols in Fig. 1 are determined as reservoir head H_R, tunnel length L_1, tunnel cross-section area A_1, head of surge tank H_s, cross-section area of surge tank A_s, penstock length L_2, penstock cross-section area A_2, tail water head H_0. Both H_R and H_0 are assumed as constants and H_0 is treated as a standard head. The conduits between the turbine and the tail water lake is assumed to be of negligible length. The water in surge tank is considered as steady flow conditions. All the symbols in this paper are with IS units.

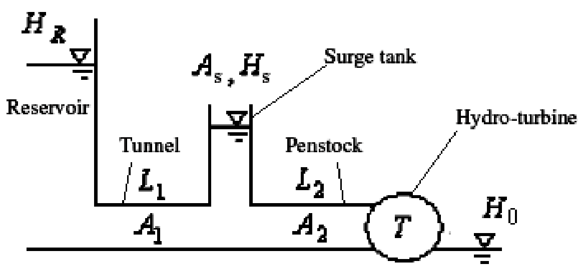

Fig. 1. Schematic of the hydraulic installation of a hydroelectric power plant with one upstream surge tank

A. Tunnel & Penstock

1) Water Hammer: The classical mass and momentum equations for one-dimensional water hammer flows in a pipe [16] are written as

$$\frac{a^2}{gA}\frac{\partial Q}{\partial l}+\frac{\partial H}{\partial t}=0 \tag{1}$$

$$\frac{1}{A}\frac{\partial Q}{\partial t}+g\frac{\partial H}{\partial l}+\frac{4}{\rho D}\tau_w=0 \tag{2}$$

where a is acoustic (waterhammer) wave speed, H is piezometric head, A is cross-sectional area of the pipe, Q is cross-sectional average flow rate, g is gravitational acceleration, D is pipe diameter, ρ is water density, τ_w is shear stress at the pipe wall, l is the spatial coordinate along the pipeline, and t is temporal coordinate. From the Darcy-Weisbach equation used in water hammer models [16], we have

$$\tau_w=\frac{\rho f||Q||Q}{8A^2} \tag{3}$$

here f is Darcy-Weisbach friction factor. If the flow rate Q from left to right is defined as positive direction, then we have (4) by substituting (3) into (2).

$$\frac{1}{A}\frac{\partial Q}{\partial t}+g\frac{\partial H}{\partial l}+\frac{fQ^2}{2gDA^2}=0 \tag{4}$$

From the mass equation (1) and the momentum equation (4), Q and H couple each other according to the viewpoint of control theory. Fang *et al* in [3] deduced the transfer function matrix of flow rate and water head of pipe inlet and outlet. In [17], the model of penstock water with elastic water hammer theory and hydraulic loss in a pipe is formulated as

$$\frac{\mathscr{L}[\mathbb{h}(t)]}{\mathscr{L}[\mathbb{q}(t)]}=-2\cdot\frac{T_w}{T_r}\cdot\tanh(\frac{T_r s}{2}+\frac{T_r H_f}{2T_w}) \tag{5}$$

where $\mathbb{h}$ is water head relative deviation of the pipe inlet and outlet, $\mathbb{q}$ is flow rate relative deviation of the pipe inlet and outlet, T_r is penstock water reflection time, H_f is hydraulic loss, L is pipe length, s is Laplace operator, $\mathscr{L}(\bullet)$ is Laplace transfer, $T_w=\frac{LQ_r}{gAH_r}$ is water inertia time, here A is cross-section area of the pipe, H_r and Q_r are rated head and rated flow rate, respectively. If penstock or tunnel is short or medium in length, then water and pipeline are taken to be incompressible. Thus, one can only consider the inelastic water hammer effect. (6) can be gotten by simplifying (5).

$$\frac{\mathscr{L}[h(t)]}{\mathscr{L}[q_(t)]}=-T_w s-H_f \tag{6}$$

2) Tunnel: In Fig. 1, water tunnel joins reservoir and surge tank together. The dynamic model of tunnel L_1 can be deduced from (6).

$$\frac{\mathscr{L}[h_1(t)]}{\mathscr{L}[q_1(t)]}=-T_{w1}s-H_{f1} \tag{7}$$

where $h_1=H_R-H_s$ is head deviation of the tunnel input and output, q_1 is flow rate deviation of the tunnel input and output, H_{f1} is hydraulic loss of the tunnel, $T_{w1}=\frac{L_1Q_r}{gA_1H_r}$ is water inertia time of the tunnel.

3) Penstock: In Fig. 1, penstock joins surge tank and tail water lake together. From (6), its dynamic model can be depicted as

$$\frac{\mathscr{L}[h_2(t)]}{\mathscr{L}[q_2(t)]}=-T_{w2}s-H_{f2} \tag{8}$$

where $h_2=H_s-H_0$ is head deviation of the penstock input and output, q_2 is flow rate deviation of the penstock input and output, $T_{w2}=\frac{L_2Q_r}{gA_2H_r}$ is water inertia time of the penstock, H_{f2} is hydraulic loss of the penstock.

B. Surge Tank

Assume no hydraulic losses at orifices of surge tank. Its equation can be derived from the continuity of flow at the two junctions.

$$T_s\frac{\mathbf{d}h_s}{\mathbf{d}t}=q_s \tag{9}$$

where h_s is water head deviation of surge tank, q_s is flow deviation of the surge tank, $T_s=\frac{A_sH_r}{Q_r}$ is filling time of surge tank.

C. Wicket Gate & Servomechanism

Gate movement is provided by a hydraulic system. The transfer function between the control signal u and the wicket gate servomotor stroke y can be expressed by a first-order equation, written as

$$\frac{\mathscr{L}[y(t)]}{\mathscr{L}[u(t)]} = \frac{1}{T_y s + 1} \tag{10}$$

here T_y is response time of wicket gate servomotor.

D. Hydro-turbine

Assume no other performance information on the turbines was available except data on net water head, full-load flow, and turbine efficiency. Then, the ideal turbine model [18] can be gotten as

$$\begin{aligned} M &= \frac{\eta \rho g H Q}{X} \\ Q &= C_t G_t \sqrt{H} \end{aligned} \tag{11}$$

Here M is the turbine torque, X is the turbine speed, and η is its efficiency at flow rate Q and water head H. ρ and g are the density of water and gravitational acceleration. C_t is the wicket gate valve coefficient and G_t is the equivalent gate position of the wicket gates in a range of 0 to 1. So that the linearized small-signal model for flow deviation q and torque deviation m of the turbine is written as

$$\begin{aligned} m &= e_x x + e_y y + e_h h \\ q &= e_{qx} x + e_{qy} y + e_{qh} h \end{aligned} \tag{12}$$

where m is turbine torque relative deviations, q is turbine flow rate relative deviations, h is turbine water head relative deviations, x is turbine speed relative deviations, y is wicket gate servomotor stroke relative deviations. The expressions of the six partial derivatives of the Francis turbine are $e_x = \frac{\partial(M/M_r)}{\partial(X/X_r)}$, $e_y = \frac{\partial(M/M_r)}{\partial(G_t/G_{\max})}$, $e_h = \frac{\partial(M/M_r)}{\partial(H/H_r)}$, $e_{qx} = \frac{\partial(Q/Q_r)}{\partial(X/X_r)}$, $e_{qy} = \frac{\partial(Q/Q_r)}{\partial G_t/G_{\max}}$, and $e_{qh} = \frac{\partial(Q/Q_r)}{\partial(H/H_r)}$, here M_r and X_r are rated turbine torque and rated speed, $G_{\max} = 1$ is the maximum equivalent gate position. These six coefficients can be obtained from (11) at an operating point. Note that e_{qx} is always zero [19].

E. Generator and Grid

Assume there is no other generation source except this hydropower plant in one grid, then the dynamic process of the generator unit with the load characteristic can be described as

$$\frac{\mathbf{d}X}{\mathbf{d}t} = \frac{M - M_{g0} - XR}{J} \tag{13}$$

here J is the moment of inertia of a unit, M is the turbine torque, M_{g0} is the electrical torque, X is the speed of the system, and R is the rotational loss coefficient. In the small-signal per-unit form, the generator and grid can be modeled as

$$\frac{\mathscr{L}[x(t)]}{\mathscr{L}[m(t) - m_{g0}]} = \frac{1}{T_a s + e_g} \tag{14}$$

here T_a is generator unit mechanical time, e_g is rotational loss coefficient. T_a is determined as $\frac{GD^2 X_r^2}{3580 P_r} \times 10^{-3}$, where GD^2 is generator unit inertia torque, P_r is generator-rated power output, X_r is rated speed.

Equations (7) – (10), (12), and (14) capture each of the individual component models of a typical hydroelectric power plant with one upstream surge tank, driven by a Francis turbine, the transfer function block diagram of which is displayed in Fig. 2. In Fig. 2, the bright blue solid means hydroelectric turbine part, the pink solid represents penstock part, the black solid depicts surge tank part, the red solid illustrates generator and grid part, and the blue solid demonstrates wicket gate and servomechanism.

III. Control Design

With the development of sensoring and measuring technology, the methods of getting data of an industrial process have been raised up, which enable us to employ the inner information of a system to achieve our control objective. As for the speed control problem of a hydroelectric turbine, we have obtained its mathematic model with a 4th-order ordinary differential equation (except the yellow part in Fig. 2), which implies that four independent state variables can depict this system from the viewpoint of modern control theory. In Fig. 2, it is obvious that the measurable variables are y, q, h, m, and x. But they are linear correlation in (12). This case indicates that only 3 independent and measurable variables can be harnessed in state space for our purpose of its control design.

Due to the advantages SMC possesses, we intend to design a sliding mode controller for governing the turbine speed. With the independent and measurable variables y, m, and x, a sliding mode controller is going to be gradually deduced. For forcing the steady state of x to tend to zero, the integral of x is utilized as an additional state x_4 with a known gain K_E [20], which is defined as

$$x_4 = K_E \int_0^{\infty} x \, \mathbf{d}t \tag{15}$$

The yellow dash in Fig. 2 shows the extra state. Then, the sliding surface takes the form as

$$S = \mathbf{c}^T \mathbf{x} \tag{16}$$

here $\mathbf{x} = [x_1 \;\; x_2 \;\; x_3 \;\; x_4]^T$, $x_1 = x$, $x_2 = m$, $x_3 = y$, $\mathbf{c} = [c_1 \; c_2 \; c_3 \; c_4]^T$, c_i $(i = 1,\ 2,\ 3,\ 4)$ is constant.

The SMC law usually includes two parts: switching control law and equivalent control law [11]. The former is employed to drive the system states moving towards a predefined sliding surface. The latter guarantees the system states keep sliding on the sliding surface and converge to the surface. During our control design, we still adopt such the approach and define the control law u as

$$u = u_{eq} + u_{sw} \tag{17}$$

Here u_{sw} is the switching control and u_{eq} is the equivalent control law, both of which expressions are deduced below. Since u_{eq} and u_{sw} are model-based, we have to obtain the reduced order model of this system. From Fig. 2, we obtain the servo component with a state x_3, the generator and grid

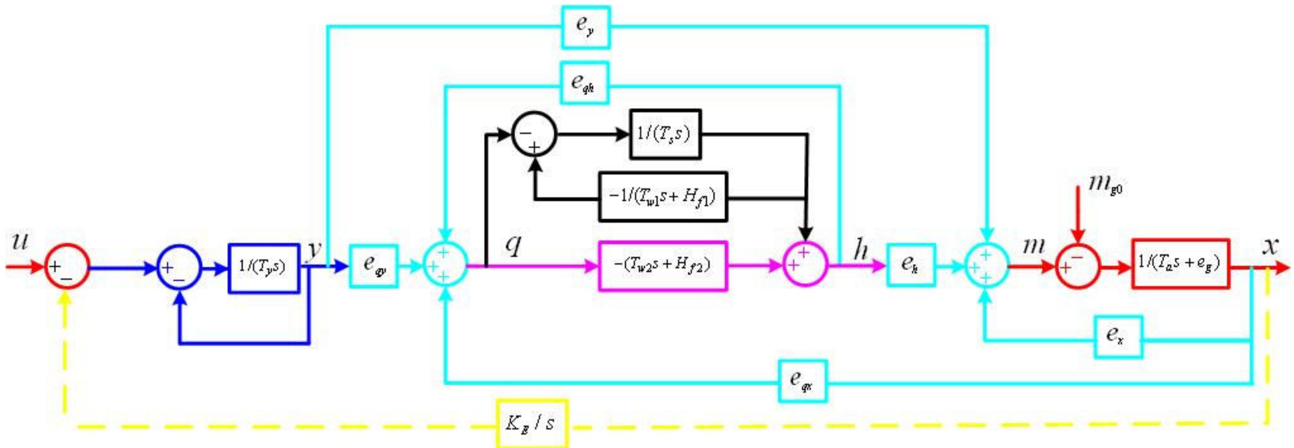

Fig. 2. Transfer function block diagram of a typical hydroelectric power plant with one upstream surge tank

component with a state x_1, and the turbine component with a linear expression. So the order of the the tunnel, surge tank and penstock components can be reduced. In Fig. 2, the transfer function of the three components is

$$\frac{\mathscr{L}[h(t)]}{\mathscr{L}[q(t)]} = -\frac{T_{w1}s+H_{f1}}{(T_{w1}s+H_{f1})T_s s+1} - T_{w2}s - H_{f2} \tag{18}$$

Since the steady value of the first term of (18) on the right is $-H_{f1}$, the reduced order model for control design can be written as

$$\frac{\mathscr{L}[h_{re}(t)]}{\mathscr{L}[q_{re}(t)]} = -T_{w2}s - H_{f2} - H_{f1} \tag{19}$$

Note that (19) are only employed for control design of the reduced order sliding mode controller. In the further simulations, (18) are still held as the model of these three components. Thus, the reduced order model of this speed governor system in state space with the state vector $\mathbf{x} = [x_1,\ x_2,\ x_3,\ x_4]^T$ can be depicted as

$$\begin{aligned} \dot{\mathbf{x}} &= \mathbb{A}\mathbf{x} + \mathbb{B}u + \mathbb{F}d(t) \\ y &= \mathbb{C}^T\mathbf{x} \end{aligned} \tag{20}$$

here state matrix $\mathbb{A}$, input vector $\mathbb{B}$, output vector $\mathbb{C}$, disturbance vector $\mathbb{F}$, disturbance sign $d(t)$ are shown in Appendix.

While the system states keep sliding on the sliding surface, only the equivalent control u_{eq} works. Differentiating S with respect to time t and letting $\dot{S} = 0$ obtain

$$\dot{S} = \mathbf{c}^T\dot{\mathbf{x}} = \mathbf{c}^T(\mathbb{A}\mathbf{x} + \mathbb{B}u_{eq}) = 0 \tag{21}$$

Substituting the nominal system of this reduced-order system (20) into (21), we have

$$u_{eq} = -(\mathbf{c}^T\mathbb{B})^{-1}\mathbf{c}^T\mathbb{A}\mathbf{x} \tag{22}$$

In order to ensure the total control law (17) makes the sliding surface (16) asymptotically stable, we define a Lyapunov function as

$$V(t) = \frac{1}{2}S^2 \tag{23}$$

Differentiating V with respect to time t and substituting (20), (17) and (22) into (23) obtain

$$\begin{aligned} \frac{\mathrm{d}V}{\mathrm{d}t} &= S\dot{S} = S[\mathbf{c}^T\dot{\mathbf{x}}] \\ &= S[\mathbf{c}^T(\mathbb{A}\mathbf{x} + \mathbb{B}u + \mathbf{c}^T\mathbb{F}d(t)\ )] \\ &= S\{\mathbf{c}^T[\mathbb{A}\mathbf{x} + \mathbb{B}(u_{eq} + u_{sw}) + \mathbf{c}^T\mathbb{F}d(t)]\} \\ &= S[\mathbf{c}^T(\mathbb{A}\mathbf{x} + \mathbb{B}u_{eq}) + \mathbf{c}^T\mathbb{B}u_{sw} + \mathbf{c}^T\mathbb{F}d(t)] \\ &= S[\mathbf{c}^T\mathbb{B}u_{sw} + \mathbf{c}^T\mathbb{F}d(t)] \end{aligned} \tag{24}$$

Let $\mathbf{c}^T\mathbb{B}u_{sw} = -\kappa S - \eta sgn(S)$ where κ and η are positive constants and $sgn(\cdot)$ is sign function, then the switching control law u_{sw} is obtained as

$$u_{sw} = -(\mathbf{c}^T\mathbb{B})^{-1}[\kappa S + \eta sgn(S)] \tag{25}$$

The control law can be obtained as

$$u = u_{eq+}u_{sw} = -(\mathbf{c}^T\mathbb{B})^{-1}[\mathbf{c}^T\mathbb{A}\mathbf{x} + \kappa S + \eta sgn(S)] \tag{26}$$

Moreover, (24) becomes

$$\begin{aligned} \frac{\mathrm{d}V}{\mathrm{d}t} &= S[-\kappa S - \eta sgn(S) + \mathbf{c}^T\mathbb{F}d(t)] \\ &\le -\kappa S^2 - \eta|S| + |S||\mathbf{c}^T\mathbb{F}d(t)| \\ &\le -\kappa S^2 - [\eta - |\mathbf{c}^T\mathbb{F}d(t)|]|S| \end{aligned} \tag{27}$$

By defining $\mathbb{D}_M = \sup|\mathbf{c}^T\mathbb{F}d(t)|$, there exist $\frac{\mathrm{d}V}{\mathrm{d}t} \le -\kappa S^2 - (\eta - \mathbb{D}_M)|S| < 0$. If $\eta > \mathbb{D}_M$ is satisfied, then the designed controller is able to stabilize the reduced order model (20).

Comment 1: For the reduced order sliding surface (16), the fulfillment of the reachability and the existence of sliding mode conditions become complicated. (16) is a reduced order system so that the sliding mode will take place in a subspace of the prototype system. With the reduced order SMC law, the reachability condition $S\dot{S} < 0$ can only ensure each element of $\mathbf{x}$ in the reduced order subspace is stable. But the stability of the reduced components, *i.e.* surge tank and tunnel, can not be held by the reduced order SMC law. So we have to analyze their stability.

Theorem 1: If the reduced order system is stable with the control law (17), then the prototype is stable as well.

Proof: From (12), we have

$$\lim_{t\to\infty}(e_x x + e_y y + e_h h) = \lim_{t\to\infty} m$$
$$\lim_{t\to\infty}(e_{qx} x + e_{qy} y + e_{qh} h) = \lim_{t\to\infty} q \tag{28}$$

As pointed out that (17) could stabilize the reduced order system, m, y, and x possess the stability, *i.e.* $\lim_{t\to\infty} m = const.$, $\lim_{t\to\infty} y = const.$, and $\lim_{t\to\infty} x = 0$. So that

$$\lim_{t\to\infty} h = const.$$
$$\lim_{t\to\infty} q = const. \tag{29}$$

which indicate q and h are still stable. So that each individual component of the speed governor system is able to stabilized by this reduced order sliding mode controller. Because the sliding mode will take place in a subspace of the prototype system, the reduced order SMC decreases the robustness of the SMC for the measurbility of the system state variables in a way. ■

IV. Simulation Results

Lubuge hydroelectric power plant, with a rated head of 312.0 m, maximum net head is 372.5 m, is on Huangni River where Yunnan and Guizhou provinces border with Guangxi Zhuang Autonomous Region, P.R. China. The installments of this plant are $4 \times 153MW$ Fracis turbines. The diversion system consists of a pressure tunnel with 9387 m in length and 8 m in diameter, a surge tank with 12 m in inner diameter and 63.9 m in height, two penstocks with 470 m in length and 4.6 m in diameter, and four branches with 3.2 m in diameter. By simplifying the branch of a turbine as its hydraulic losses, our mathematic model with surge tank is able to depict the operating condition while one penstock supplies a solitary turbine. So that the data of this plant are employed to simulate for load rejection. The data of the generation unit of this plant are determined as $P_r = 153\ MW$, $H_r = 312.0\ m$, $Q_r = 53.5\ m^3$, $X_r = 333.3\ r/min$, $L_1 = 9387\ m$, $A_1 = 49.6\ m^2$, $A_s = 113.04\ m^2$, $L_2 = 470\ m$, $A_2 = 16.61\ m^2$, $GD^2 = 4.0 \times 10^4\ kN \cdot m^2$. Under our operating condition that is one penstock supplying one turbine, $H_{f1} = 0.036$ and $H_{f2} = 0.027$. The time constants T_a, T_y, T_{W1}, T_{W2}, and T_s are gotten as 8.113, 0.500, 3.312, 1.244, and 659.224, respectively. Assume this hydroelectric generating unit is connected to an isolated system. The turbine coefficients under the operating condition case 1 and case 2 are determined as Table I. K_E is picked up as 0.200. The parameter of the reduced order sliding surface on the operating point Case 1 in Table I is gotten as $\mathbf{c} = [500\ 35\ 63\ 600]^T$ from Acker command of MATLAB by placing the pole of Ackermanns formula in the specified vector $[-1\ \ -2-2i\ \ -2+2i\ \ -9]^T$. κ and η are selected as 1.00 and 0.500.

A. Load Rejection

Fig. 3 illustrates the comparison of 10% load rejection under the operating condition Case 1 by the reduced order SMC and PID governor, where the PID gains are tuned as $K_p = 0.85$, $K_i = 3$, and $K_d = 2$ [21]. Displayed in Fig. 3, the presented governor possesses a better performance than the conventional PID controller from the viewpoint of speed deviations x. Compared with the slow response of the PID governor, the wicket gate deviation y under the action of the reduced order SMC governor can respond the minute that the load changes. Correspondingly, the flow deviation q is changed to regulate the unit power. So that x can be rectified as soon as possible. Further, we can also explain the reason that the presented control method possesses the better performance from the viewpoint of information. The reduced order SMC makes full use of the system information and the extra state to decide the final control u, whereas, the PID controller employs the proportional, integral, and derivative of x to formulate the final control u, only utilizing a part of the system information.

TABLE I
TURBINE COEFFICIENTS FOR STEADY-STATE OPERATING POINTS

	e_x	e_y	e_h	e_{qx}	e_{qy}	e_{qh}	e_g
Case 1	-1.000	1.000	1.500	0.000	1.000	0.500	0.210
Case 2	-0.260	0.322	0.722	0.000	0.573	0.325	0.210

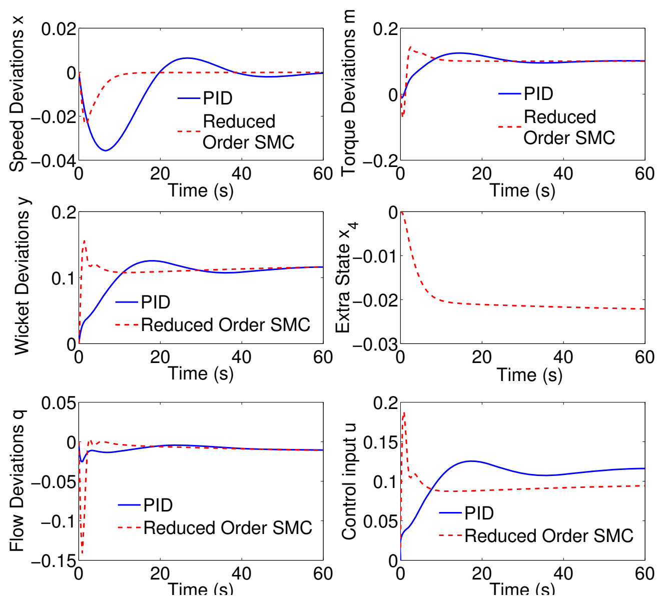

Fig. 3. Simulation results of 10% load rejection under the operating condition Case 1 by the reduced order sliding mode governor, compared with PID governor

B. Robustness Testing

Fig. 4 demonstrates the results of robustness testing of 10% load rejection under the operating condition Case 1 and Case 2, by the same controller parameters. As shown in Fig. 4, the presented controller can still hold a robust performance even when it operates under the different operating condition. Due to the adopted robust control method, the presented governor earns a robust performance. This is very meaningful for the safe and economical operation of hydroelectric power plants.

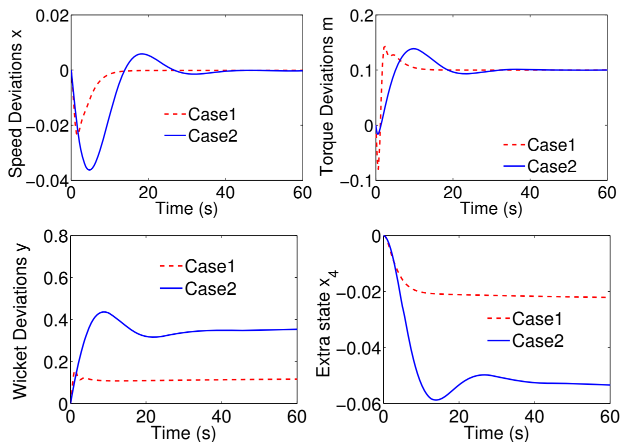

Fig. 4. Simulation results of 10% load rejection under the different operating conditions, Case 1 and Case 2, by the same controller parameters

V. Conclusions

This paper has presented a reduced order sliding mode controller to govern the speed of a hydroelectric turbine. The model of a hydroelectric power plant with one upstream surge tank is built up at first. By introducing an additional state variable, a reduced order sliding mode controller is presented for the speed governor of this power plant. From our proof, this reduced order controller possesses the ability to stabilize the prototype system. For searching the optimized parameters of the reduced order sliding surface, genetic algorithm is employed. Finally, simulation results show the feasibility and robustness of the presented governing method.

The two main contributions of this paper are to model a hydroelectric power plant with one upstream surge tank & a penstock, and to present a reduced order sliding mode control method. How to model a hydroelectric power plant with a surge tank & more penstocks and to design its controller are still continuous research field.

Appendix

Under the operating condition Case 1 in Table I, the matrices $\mathbb{A}$, $\mathbb{B}$, $\mathbb{C}$, and $\mathbb{F}$ in our example are determined as

$$\mathbb{A} = \begin{bmatrix} -0.149 & 0.123 & 0 & 0 \\ -0.939 & -1.109 & 3.425 & 2.488 \\ 0 & 0 & -2.000 & -2.000 \\ 0.200 & 0 & 0 & 0 \end{bmatrix}$$

$$\mathbb{B} = [0 \ \ -2.488 \ 2.000 \ 0]^T$$

$$\mathbb{C} = [1 \ 0 \ 0 \ 0]^T$$

$$\mathbb{F} = [-0.123 \ 0.077 \ 0 \ 0]^T$$

References

[1] Grubb, M., Butler, L., and Twomey, P. Diversity and security in UK electricity generation: The influence of low-carbon objectives, *Energy Policy*, 2006, 34(18), 4050 - 4062.

[2] Kishor, N., Saini, R.P., and Singh, S.P. A review on hydropower plant models and control, *Renewable and Sustainable Energy Reviews*, 2007, 11(5), 776 - 796.

[3] Fang, H.Q., Chen, L., Dlakavu, N., and Shen, Z.Y. Basic Modeling and Simulation Tool for Analysis of Hydraulic Transients in Hydroelectric Power Plants, *IEEE Transactions on Energy Conversion*, 2008, 23(3), 834 - 841.

[4] Natarajan, K. Robust PID Controller Design for Hydroturbines, *IEEE Transactions on Energy Conversion*, 2005, 20(3), 661 - 667.

[5] Jiang, C.W., Ma, Y.C., and Wang, C.M. PID controller parameters optimization of hydro-turbine governing systems using deterministic-chaotic-mutation evolutionary programming (DCMEP), *Energy Conversion and Management*, 2006, 47(9-10), 1222 - 1230.

[6] Jones, D. and Mansoor, S. Predictive feedforward control for a hydroelectric plant, *IEEE Transactions on Control Systems Technology*, 2004, 12(6), 956 - 965.

[7] Kishor, N. and Singh, S.P. Simulated response of NN based identification and predictive control of hydro plant, *Expert Systems with Applications*, 2007, 32(1), 233 - 244.

[8] Mahmoud, M., Dutton, K., and Denman, M. Design and simulation of a nonlinear fuzzy controller for a hydropower plant, *Electric Power Systems Research*, 2005, 73(2), 87 - 99.

[9] Jiang, J. Design of an optimal robust governor for hydraulic turbine generating units, *IEEE Transactions on Energy Conversion*, 1995, 10(1), 188 - 194.

[10] Salhi, I., Doubabi, S., Essounbouli, N., and Hamzaoui, A. Application of multi-model control with fuzzy switching to a micro hydro-electrical power plant, *Renewable Energy*, 2010, 35(9), 2071 - 2079.

[11] Utkin, V.I. *Sliding Modes in Control and Optimization*. New York, USA: Springer-Verlag, 1992.

[12] Erschler, J., Roubellat, F., and Vernhes, J.P. Automation of a hydroelectric power station using variable-structure control systems, *Automatica*, 1974, 10(1), 31 - 36.

[13] Ye, L.Q., Wei, S.P., Xu, H.B., Malik, O.P., and Hope, G.S. Variable structure and time-varying parameter control for hydroelectric generating unit, *IEEE Transactions on Energy Conversion*, 1989, 4(3), 293 - 299.

[14] Jing, L., Ye, L.Q., Malik, O.P., and Zeng, Y. An intelligent discontinuous control strategy for hydroelectric generating unit, *IEEE Transactions on Energy Conversion*, 1998, 13(1), 84 - 89.

[15] IEEE Committee Report, "Hydraulic turbine and turbine control models for system dynamic studies," *IEEE Transactions on Power Systems*, 1992, 7(1), 167 - 178.

[16] Ghidaoui, M.S. , Zhao, M., McInnis, D.A., Axworthy, D.H., and McInnis, D. A. A review of water hammer theory and practice, *Applied Mechanics Reviews*, 2005, 58(1), 49 -76.

[17] Sanathanan, C.K. Accurate Low Order Model for Hydraulic Turbine-Penstock, *IEEE Transactions on Energy Conversion*, 1987, EC-2(2), 196 - 200.

[18] Streeter, V.L., and Wylie, B.E. *Fluid Mechanics*, New York: McGraw-Hill, 1979.

[19] Doan, R.E., and Natarajan, K. Modeling and control design for governing hydroelectric turbines with leaky Wicket gates, *IEEE Transactions on Energy Conversion*, 2004, 19(2), 449 - 455.

[20] Tan, W. and Xu, Z. Robust analysis and design of load frequency controller for power systems, *Electric Power Systems Research*, 2009, 79(5), 846 - 853.

[21] Stein, T. Frequency control under Isolated network conditions, *Water Power*, 1970.